Species-specific response to climate reconstruction in upper-elevation mixed-conifer forests of the western Sierra Nevada, California

Matthew Hurteau, Harold Zald, and Malcolm North

Abstract: Dendrochronology climate reconstruction studies often sample dominant, open-grown trees to reduce competition effects and isolate annual climate influences on radial increment growth. However, there has been no examination of how species respond as stand densities increase or which species in mixed-conifer forests provide a better record of past climate. We sampled 579 trees representing five upper montane mixed-conifer species at the Teakettle Experimental Forest in California's southern Sierra Nevada to determine species-specific responses to annual climatic fluctuations. Using the Kalman filter, we examined the affect of local stand density on growth response and whether the growth–climate relationship improved with a time lag. The Kalman filter iteratively calculates error for predicted versus actual radial growth and accounts for this variation in the corrector equation. Under current high-density conditions, shade-tolerant white fir (*Abies concolor* (Gord. & Glend.) Lindl.) provided the best model for climate reconstruction. Shade-intolerant Jeffrey pine (*Pinus jeffreyi* Grev. & Balf.) had a lagged response to annual climatic fluctuations, possibly because its roots may tap water reserves in granitic bedrock fissures. Open-grown trees provided more accurate records of climate. Changes in forest density in this forest may have resulted in changes in species-specific response to annual climatic fluctuations.

Résumé : Les études de reconstitution du climat à l'aide de la dendrochronologie échantillonnent souvent des arbres dominants croissant à découvert pour réduire les effets de la compétition et isoler l'influence annuelle du climat sur la croissance radiale. Cependant, aucune étude n'a cherché à déterminer de quelle façon réagissent les différentes espèces à l'augmentation de la densité du peuplement ou quelle espèce témoigne le mieux du climat passé dans les forêts mixtes de conifères. Nous avons échantillonné 579 arbres représentant cinq espèces de conifères de forêt mixte de haute montagne à la Forêt expérimentale de Teakettle, dans la partie sud de la Sierra Nevada en Californie, pour déterminer les réactions de chaque espèce aux fluctuations annuelles du climat. À l'aide du filtre de Kalman, nous avons examiné l'effet de la densité locale du peuplement sur la réponse en croissance et déterminé si la relation entre le climat et la croissance s'améliorait avec un décalage dans le temps. Le filtre de Kalman calcule par itération l'erreur de la croissance radiale prédite relativement à la croissance radiale réelle et tient compte de cette variation dans l'équation de correction. Dans les conditions actuelles de forte densité, le sapin concolore (*Abies concolor* (Gord. & Glend.) Lindl.), une espèce tolérante à l'ombre, constituait le meilleur modèle pour la reconstitution du climat. Le pin de Jeffrey (*Pinus jeffreyi* Grev. & Balf.), une espèce intolérante à l'ombre, avait une réaction décalée aux fluctuations annuelles du climat, possiblement parce que ses racines ont accès aux réserves d'eau dans les fissures du substratum granitique. Les arbres qui croissent à découvert fournissent les données les plus justes sur le climat. Les changements dans la densité de cette forêt pourraient avoir entraîné des changements dans les réactions aux fluctuations annuelles du climat propres à chaque espèce.

[Traduit par la Rédaction]

Introduction

Tree-ring climate reconstructions have been an important tool for providing site-specific records of climatic fluctuations where long-term instrumental data are unavailable. Often, these reconstructions are based on measurements from dominant trees and sites that are preferentially selected to avoid trees affected by competitive stand dynamics. Standard reconstruction methods rely on the principle of uniformitarianism, which states that tree growth response to current and past climate conditions will be similar. The uniformitarian assumption, however, may not hold for closed-canopy forest conditions (Van Deusen and Koretz 1988), where density-dependent competition can override the relationship between tree growth and climate. With the advent of fire suppression, many old trees in western forests are no

Received 19 July 2006. Accepted 7 February 2007. Published on the NRC Research Press Web site at cjfr.nrc.ca on 28 September 2007.

M. Hurteau.[1,2] Department of Plant Sciences, University of California, Davis, CA 95616, USA; USDA Forest Service, Sierra Nevada Research Center, 2121 2nd Avenue, Suite A-101, Davis, CA 95616, USA.
H. Zald.[3] USDA Forest Service, Pacific Northwest Research Station, 3200 SW Jefferson Way, Corvallis, OR 97331, USA.
M. North. USDA Forest Service, Sierra Nevada Research Center, 2121 2nd Avenue, Suite A-101, Davis, CA 95616, USA.

[1]Corresponding author (e-mail: Matthew.Hurteau@nau.edu).
[2]Present address: Northern Arizona University, Box 6077, Flagstaff, AZ 86011, USA.
[3]Present address: College of Forestry, Oregon State University, Corvallis, OR 97331, USA.

 doi:10.1139/X07-028

longer growing in open conditions and may be experiencing decreased basal area increment because of resource competition (Biondi 1996). A shift in the late 19th century climate that is causing a general warming trend may be resulting in a decreased tree growth response to climate (Wilmking et al. 2004; Briffa et al. 1998*a*); however, no consensus currently exists on tree growth response to climate change (Pan and Raynal 1995). Given this change in forest conditions, alternative methods of tree-ring analysis are needed to identify which species and individuals in high-density mixed stands provide the best correlation between radial increment growth and annual climate conditions.

State-space models offer an alternative analysis of radial increment growth that can be used to track growth trends over time and do not rely on uniformitarianism. One model, the Kalman (1960) filter, iteratively optimizes its predictive estimates and minimizes the estimated error covariance (Maybeck 1979). This iterative process accounts for all data points up to and including data from the previous time step, but the recursive methodology effectively gives more weight to recent data and less weight to past data (Van Deusen and Koretz 1988) when predicting the next time step. In the iterative process, the amount of error in the predicted versus the actual data point is calculated, the error is accounted for, and a corrector equation is applied to minimize the estimated error covariance in the next time step. The Kalman filter does not rely on the uniformitarian assumption, because the error covariance can change with each time step enabling the climate reconstruction to compensate for climatic shifts and changes in forest density that can affect the growth–climate relationship for tree rings. The Kalman filter has been used extensively in electrical, computer, and aerospace engineering (Shumway and Stoffer 2000; Maybeck 1979) and has recently been applied in ecology to reconstruct productivity in salmon (Peterman et al. 2003), to monitor growth of American beech (*Fagus grandifolia* Ehrh.) affected by beech bark disease (Gove and Houston 1996), and to examine tree-ring response to climate and pollution (Pan and Raynal 1995; van den Brakel and Visser 1996; Van Deusen and Koretz 1988; Van Deusen 1990). To date, the Kalman filter has never been applied to a tree-ring data set for a multispecies, closed-canopy stand where radial increment growth will likely vary among species and over time following fire suppression.

The upper mixed-conifer forest in California's southern Sierra Nevada has five main species and has significantly changed from an open parklike stand structure, as described by Muir (1894), to closed-canopy conditions as a result of fire suppression (McKelvey and Busse 1996) and other human caused disturbances, such as livestock grazing (Stephens and Elliot-Fisk 1998). In this Mediterranean climate with a prolonged summer drought, available water derived from the winter snowpack is the most significant influence on growth (Witty et al. 2003). Within mixed-conifer forest, species abundance varies with microsite conditions. Red fir (*Abies magnifica* A. Murr.) is usually concentrated in riparian corridors and cold air drainages; white fir (*Abies concolor* (Gord. & Glend.) Lindl.), incense cedar (*Calocedrus decurrens* (Torr.) Florin), and sugar pine (*Pinus lambertiana* Dougl.) occur in midslope areas; and Jeffrey pine (*Pinus jeffreyi* Grev. & Balf.) is found in shallow soils on ridgetops (North et al. 2002). Some studies have suggested microsite differences in soil and bedrock fissure water-holding capacity may buffer or lag Jeffrey pine's susceptibility to a given year's climate conditions (Arkley 1981, Hubbert et al. 2001). Unmanaged Sierran mixed-conifer forests are multiaged, have a clustered stem distribution, and have experienced a century of fire suppression that could alter species and individual growth response to climate. Our objective was to determine which of the five species in mixed-conifer forest is the most responsive to nonlagged and time-lagged climatic fluctuations. Specifically, our hypotheses were (*i*) there will be significant differences between species in their radial growth response to fluctuations in annual climate as measured by Palmer drought severity index (PDSI) (Palmer 1965; Cook et al. 1999); (*ii*) for all species, the model of increment growth and annual climate will be better for current year than any of the time-lagged models; and (*iii*) amongst trees of the same species, there will be a significantly better fit of radial growth with climate for individuals growing in open versus closed stand conditions.

Tree-ring records have been a powerful tool for reconstructing past climate conditions, but to date, there have been no studies comparing different tree species within Sierran mixed-conifer stands or assessing how local density may affect the correlation between annual climate and radial growth increment.

Methods

Study area

This study was conducted at the 1300 ha Teakettle Experimental Forest, southern Sierra Nevada, California (http://teakettle.ucdavis.edu). An old-growth forest, ranging between 1900 and 2600 m in elevation, Teakettle is located 80 km east of Fresno, California, on the north fork of the Kings River. The Experimental Forest consists of forest types ranging from mixed conifers at lower elevations to a mix of red fir and lodgepole pine (*Pinus contorta* Dougl. ex Loud. var. *latifolia* Engelm.) at higher elevations. We sampled 579 trees in the mixed-conifer forest. By basal area, the mixed-conifer portion of the experimental forest is 60% white fir, 18% incense cedar, 13% sugar pine, 4% Jeffrey pine, 4% red fir, and 1% hardwoods (North et al. 2004).

Tree rings

Sampling was conducted within a 200 ha contiguous block of mixed-conifer forest. The long-term Teakettle project is a 3 × 2 full factorial design, comparing the effects of thinning and burning on 18 replicated 4 ha plots (North et al. 2002). Within this experimental framework, we used a postharvest, opportunistic sampling strategy to collect cross sections from stumps. We utilized this sampling methodology to overcome sampling bias that can occur by sampling only dominant and codominant individuals (Steele and Fiedler 1996). A subset of six thinned plots was selected; within the plots, all stumps that were accessible and safe to sample with a chainsaw were selected. From the subset of six plots, 579 individual trees were sampled. Of these 579 individuals, we excluded samples with rot and were able to use 538, of which 292 (54%) were white fir, 63 (12%) were red fir, 99 (18%) were incense cedar, 35 (7%) were Jeffrey

Fig. 1. Tree series sample numbers over time used to develop master chronologies.

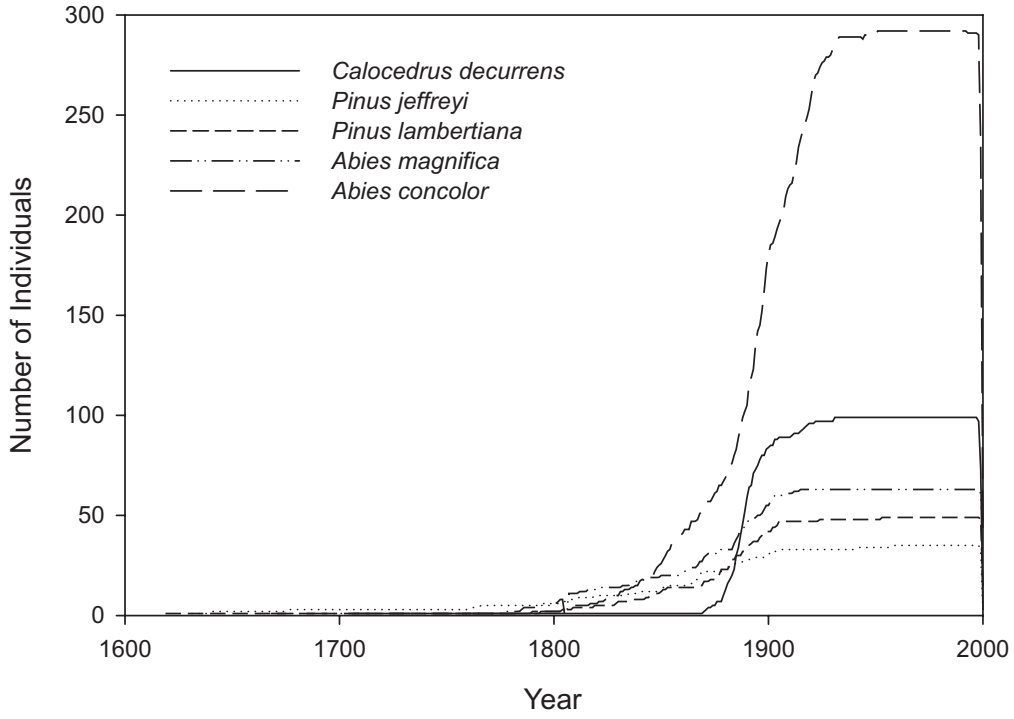

pine, and 49 (9%) were sugar pine. Organic matter was removed from the base of stumps and cross sections were cut at mineral soil depth. Cross sections were sanded and cut into strips cambium to cambium, and aged prior to cross dating. We began with what appeared to be the 20 oldest cross sections. The cross sections were skeleton plotted and cross-dated as described by Stokes and Smiley (1968). Marker years of narrow growth were identified from these initial cross-dated samples. These marker years were then used as a reference list for comparing all other series, which were cross-dated using methods described by Yamaguchi (1991). After cross dating, cross sections were aged again, and corrections made to original sample age estimates.

Annual ring width was measured to the nearest 0.001 mm using a Unislide "TA" tree-ring measuring system (Velmex, Bloomfield, New York). Chronologies and sample depth over time were constructed for each species (Fig. 1). Chronologies were developed for each species to remove low-frequency growth variability using the software ARSTAN (Holmes et al. 1986). Detrending started by applying a negative exponential curve or linear regression (whichever had the best fit) to the raw tree-ring series of each tree. Residual indices were computed by subtracting the growth values from the detrending curve or line. A cubic smoothing spline was not applied, because the removal of growth trends is user defined and risks the loss of variability that may be derived from long-term climate trends (Briffa and Osborn 1999). Chronology computation from each ring series was accomplished by using a robust biweighted mean. Residual chronologies were produced using the residuals from autoregressive modeling of the standard chronologies. Each series was modeled as an autoregressive process, where the order was selected for the individual series by a first-minimum Akaike information criterion (AIC) search (Akaike 1973). We examined residual chronology descriptive statistics using series correlations to the chronology and sensitivity indices (Table 1).

Table 1. Residual chronology descriptive statistics including series correlations to the chronology and sensitivity indices.

Species	Mean corrlations among all radii	Mean sensitivity
Abies concolor	0.1795	0.3571
Abies magnifica	0.083	0.4517
Calocedrus decurrens	0.2	0.3273
Pinus jeffreyi	0.179	0.513
Pinus lambertiana	0.16	0.5403

Weather records

To assess whether local (i.e., Teakettle) climate patterns corresponded with regional (i.e., PDSI) climate measures, we used the same nested calibration approach used by North et al. (2005). This method involved gathering climate records from Grant Grove (the closest long-term climate monitoring station, 20 km away at the same 1800 m elevation), which had snow records dating back to 1930, and precipitation records dating back to 1878 from Fresno, California (80 km away and at 50 m elevation). Then, we calculated water year totals (1 July – 30 June) and standardized each data set by subtracting the mean and dividing by the standard deviation. Comparing Grant Grove snow records with three widely cited El Niño – La Niña sources that agreed on events over the past 30 years (Kiladis and Diaz 1989; Smith and Sardeshmukh 2000; NOAA Climate Prediction Center, http://www.cpc.ncep.noaa.gov) we found that years that were one standard deviation above and below the mean match El Niño and La Niña events. We then compared the Grant Grove data set to the Fresno data set and determined

precipitation thresholds that signified El Niño and La Niña events. Identifying these thresholds allowed us to identify potential events between 1878 and 1929. Next we compared these data with the North American drought variability (PDSI) reconstructions (we used the grid point nearest Teakettle: 37°N, 119.5°W, 25 km away), which had values for 1700–1978 (Cook et al. 1999). We found that local El Niño – La Niña events corresponded to every El Niño – La Niña event in the PDSI. Although PDSI reconstructs climate from 400 different tree-ring series and is only a proxy for past climatic conditions, the comparisons with local climate records suggest a reasonable correspondence between past Teakettle climate and PDSI values.

Relative density

We calculated an approximation of local crowding for each sample tree using Thiessen polygons. The size and distribution of Thiessen polygons has been used to evaluate the impact of density, growing space, and competition of neighboring plants on plant succession (Mithen et al. 1984; Kenkel et al. 1989). All trees ≥5 cm diameter at breast height (DBH), including our 538 sample trees, were mapped using a surveyor's total station for the Teakettle Experiment. Using this stem map and ARC/INFO software, the area around each tree was bisected by an equidistant line between adjacent stem locations, and the lines were connected to form a polygon around each cookie-sampled tree location (Kenkel et al. 1989). The polygon's area is an approximation of the potential growing space, in square metres, for an individual tree. Polygon size is a function of local stand density, with smaller areas indicative of dense, "dog hair" conditions. Polygons were then weighted by dividing each polygon's area by the basal area in square metres of the individual tree to take into account the greater growing space demands (i.e., light, water, and nutrients) of larger trees. This approximation of local stand density is limited, because it is estimated from current conditions.

Analysis

To examine species-specific response to climate and the resultant climate reconstruction differences, we used the Kalman filter, which forecasts time (t) using all information at time $t - 1$ (Gove and Houston 1996; Shumway and Stoffer 2000; Van Deusen and Koretz 1988). As new information becomes available, the estimate is recursively updated (du Plessis 1996). To use a linear model with the Kalman filter, the model is written in state-space form represented by the observation and transition equations:

$$[1] \qquad Y_t = \mathbf{X}_t\boldsymbol{\alpha}_t + \boldsymbol{v}_t$$

$$[2] \qquad \boldsymbol{\alpha}_t = \mathbf{G}_t\boldsymbol{\alpha}_{t-1} + \boldsymbol{w}_t$$

where Y_t is an estimate of the mean ring width, $\mathbf{X}_t$ is a matrix of lagged ring widths (taken from each species master chronology and PDSI values), $\boldsymbol{\alpha}_t$ is a state vector, $\boldsymbol{v}_t$ is a white noise vector resulting from the inability to directly measure the state variable $\boldsymbol{\alpha}_t$, $\mathbf{G}_t$ is a transition matrix, and $\boldsymbol{w}_t$ is an error vector.

State-parameter estimates are made using three sets of equations: prediction, updating, and smoothing equations (Van Deusen and Koretz 1988). Following Van Deusen and Koretz (1988), an optimal estimation (a_t) is calculated for $\boldsymbol{\alpha}_t$. This estimation includes all information up to and including Y_t.

$$[3] \qquad a_{t/t-1} = \mathbf{G}_t a_{t-1}$$

$$[4] \qquad \mathbf{P}_{t/t-1} = \mathbf{G}_t\mathbf{P}_{t-1}\mathbf{G'}_t + \mathbf{W}_t$$

where $\mathbf{P}_t$ is the covariance matrix of $a_t - \boldsymbol{\alpha}_t$ and $\mathbf{W}_t$ is the transition variance matrix. As follows, when Y_t becomes available, the updating equations for estimating $\boldsymbol{\alpha}_t$ and the associated covariance matrix are

$$[5] \qquad a_t = a_{t/t-1} + \mathbf{P}_{t/t-1}\mathbf{X'}_t\mathbf{H}_t^{-1}E_t$$

$$[6] \qquad \mathbf{P}_t = \mathbf{P}_{t/t-1} - \mathbf{P}_{t/t-1}\mathbf{X'}_t\mathbf{H}_t^{-1}\mathbf{P}_{t/t-1}$$

where E_t is a weighted mean of the prediction errors and H_t is the covariance matrix of those prediction errors, which are calulated as follows:

$$[7] \qquad E_t = Y_t - \mathbf{X}_t a_{t/t-1}$$

$$[8] \qquad \mathbf{H}_t = \mathbf{X}_t\mathbf{P}_{t/t-1}\mathbf{X'}_t + \mathbf{V}_t$$

where $\mathbf{V}_t$ is equal to the variance of $\boldsymbol{v}_t$. $\mathbf{V}_t$ and $\mathbf{W}_t$ are calculated using q parameters and σ_t^2. The among-tree variance σ_t^2 from the standardized master chronology is used to estimate σ_t^2, and maximum likelihood is used to estimate the unknown q parameters (see Van Deusen and Koretz 1988).

The AIC was used to select the species-specific model that most accurately predicts PDSI. We used AIC_c, a correction for small sample size (Burnham and Anderson 2002). AIC_c requires an estimate of maximum likelihood (L), which was calculated using

$$[9] \qquad L = -0.5\sum \ln|\mathbf{H}_t| + E'_t\mathbf{H}_t^{-1}E_t$$

where new information in Y_t is represented by E_t. Using the following formula, we computed AIC_c as well as Δ_i (the difference between the lowest AIC_c value and the AIC_c value for a given model i; it is used to rank models and determine the level of empirical support), w_i (the weight of evidence; another metric for model selection, calculated by dividing the model likelihood for a given model by the sum likelihoods), and w_i/w_j (the evidence ratio for each model; the ratio of the weights of evidence of the best model and a given model)

$$[10] \qquad AIC_c = 2L + 2k + \frac{2(k+1)(k+2)}{T-k-2}$$

where k is the number of state parameters plus the number of q parameters.

Different models were evaluated using Δ_i following Burnham and Anderson (2002). Models having a Δ_i within 2 of the best model are substantially supported, whereas models having a Δ_i between 4 and 7 have considerably less support. Approximate 95% confidence intervals were calculated for the filtered response of each species using plus or minus two times the square root of the variance estimates of

Table 2. The MVNR, AIC_c, Δ_i, w_i, and evidence ratio values for the five species-specific climate models ranked by AIC_c value.

Species	MVNR[a]	MVNR 95% CI	C^*[b]	$P(C^*)$	AIC_c[c]	Δ_i[d]	w_i[e]	Evidence ratio[f]
Abies concolor	2.026	1.796–2.204	–0.053	0.468	–5.013	0	0.539	
Calocedrus decurrens	2.165	1.796–2.204	–0.036	0.549	–0.908	4.104	0.069	7.872
Pinus lambertiana	2.104	1.796–2.204	0.033	0.534	–0.639	4.374	0.060	8.910
Abies magnifica	2.005	1.796–2.204	–0.013	0.824	0.084	5.098	0.042	12.798
Pinus jeffreyi	2.107	1.796–2.204	0.025	0.633	2.576	7.590	0.012	44.487

Note: Models with a Δ_i within 2 of the best model have equal support. A Δ_i between 4 and 7 indicates considerably less support.
[a]Modified Von Neumann ratio and 95% confidence intervals.
[b]The C^* indicates model misspecification if $P(C^*)$, the probability of a greater absolute value of C^*, is small.
[c]Akaike's information criterion adjusted for small sample size.
[d]Δ AIC_c values.
[e]Weight of evidence and percentage of weight represented by given model.
[f]The ratio of weights of a given model and the best model.

Table 3. The MVNR, AIC_c, Δ_i, w_i, and evidence ratio values for the six lagged climate models for Jeffrey pine ranked by AIC_c value.

Time lag (years)	MVNR[a]	MVNR 95% CI	C^*[b]	$P(C^*)$	AIC_c[c]	Δ_i[d]	w_i[e]	Evidence ratio[f]
5	2.076	1.794–2.205	0.029	0.589	–1.040	0	0.210	
2	2.094	1.794–2.205	0.032	0.543	–1.038	0.001	0.210	1.001
10	2.071	1.794–2.205	0.027	0.615	–0.922	0.118	0.198	1.061
3	2.096	1.794–2.205	0.031	0.564	–0.833	0.207	0.189	1.109
1	2.098	1.794–2.205	0.032	0.548	0.018	1.059	0.123	1.698
15	2.061	1.794–2.205	0.029	0.593	1.209	2.249	0.068	3.080
0	2.107	1.796–2.204	0.025	0.633	2.576	3.617	0.033	6.102

Note: Models with a Δ_i within 2 of the best model have equal support. An added time lag 0 model is given for reference.
[a]Modified Von Neumann ratio and 95% confidence intervals.
[b]The C^* indicates model misspecification if $P(C^*)$, the probability of a greater absolute value of C^*, is small.
[c]Akaike's information criterion adjusted for small sample size.
[d]Δ AIC_c values.
[e]Weight of evidence and percentage of weight represented by given model.
[f]The ratio of weights of a given model and the best model.

the q parameters. In addition, we calculated the modified Von Neumann ratios (MVNR) and their 95% confidence intervals and ran the C^* test. MVNR uses the recursive residuals to test whether the prediction errors are independent, and C^* is a test statistic using the recursive residuals to determine whether the model is correctly specified (see Van Deusen 1990). C^* has a t distribution when the model is correctly specified.

For each species, we developed models of radial increment growth against a time lag of PDSI values. We lagged the tree ring chronologies by 1, 2, 3, 5, 10, and 15 years and modeled them against the PDSI data set using AIC_c to evaluate the performance of the different lag periods. The time lag models were arbitrarily selected to explore the idea that an abiotic factor may be acting on each species, thereby resulting in a delayed response to annual climatic variation.

To analyze the potential effects of tree density, radial growth, and climate response, we ran Kalman filters for a subset of 46 trees that represented a range of Thiessen values within each species and calculated their corresponding AIC_c values. We plotted AIC_c values against weighted Thiessen polygon size for each species and used dummy variable regression to examine whether there was a polygon size threshold at which AIC_c values rapidly increased. After identifying the threshold value, we ran filters for all individuals that had Thiessen values greater than or equal to the threshold value.

Results

Model selection — Species-specific response

All model prediction errors were determined to be independent based on their associated MVNR values falling within the 95% confidence intervals (Tables 2 and 3). The C^* test statistics and their associated p values indicate that all models were correctly specified (Tables 2 and 3). We identified differences between the fit of annual increment and PDSI values for mixed conifer's five species. White fir had the lowest AIC_c value of –5.01 (Table 2) and the greatest number of occurrences where actual PDSI measurements fell within the 95% confidence intervals ($2 \pm \sqrt{1.10429}$) (Fig. 2*a*). White fir also represented 53% of the total weight (w_i) among models (Table 2). Incense cedar, sugar pine, and red fir had AIC_c values of –0.90, –0.63, and 0.08, respectively (Table 2). The Δ_i values for incense cedar (4.1; Fig. 2*c*), sugar pine (4.3; Fig. 2*e*), and red fir (5.0; Fig. 2*b*) fell between 4 and 7, indicating considerably less support for the models (Burnham and Anderson 2002). Jeffrey pine had an AIC_c value of 2.57 with Δ_i equal to 7.5 (Fig. 2*d*).

Fig. 2. Kalman filter predictions (solid line) with 95% confidence intervals (broken lines) and PDSI values (●) plotted over time for the five principle species in the mixed-conifer forest: (*a*) white fir, (*b*) red fir, (*c*) incense cedar, (*d*) Jeffrey pine, and (*e*) sugar pine.

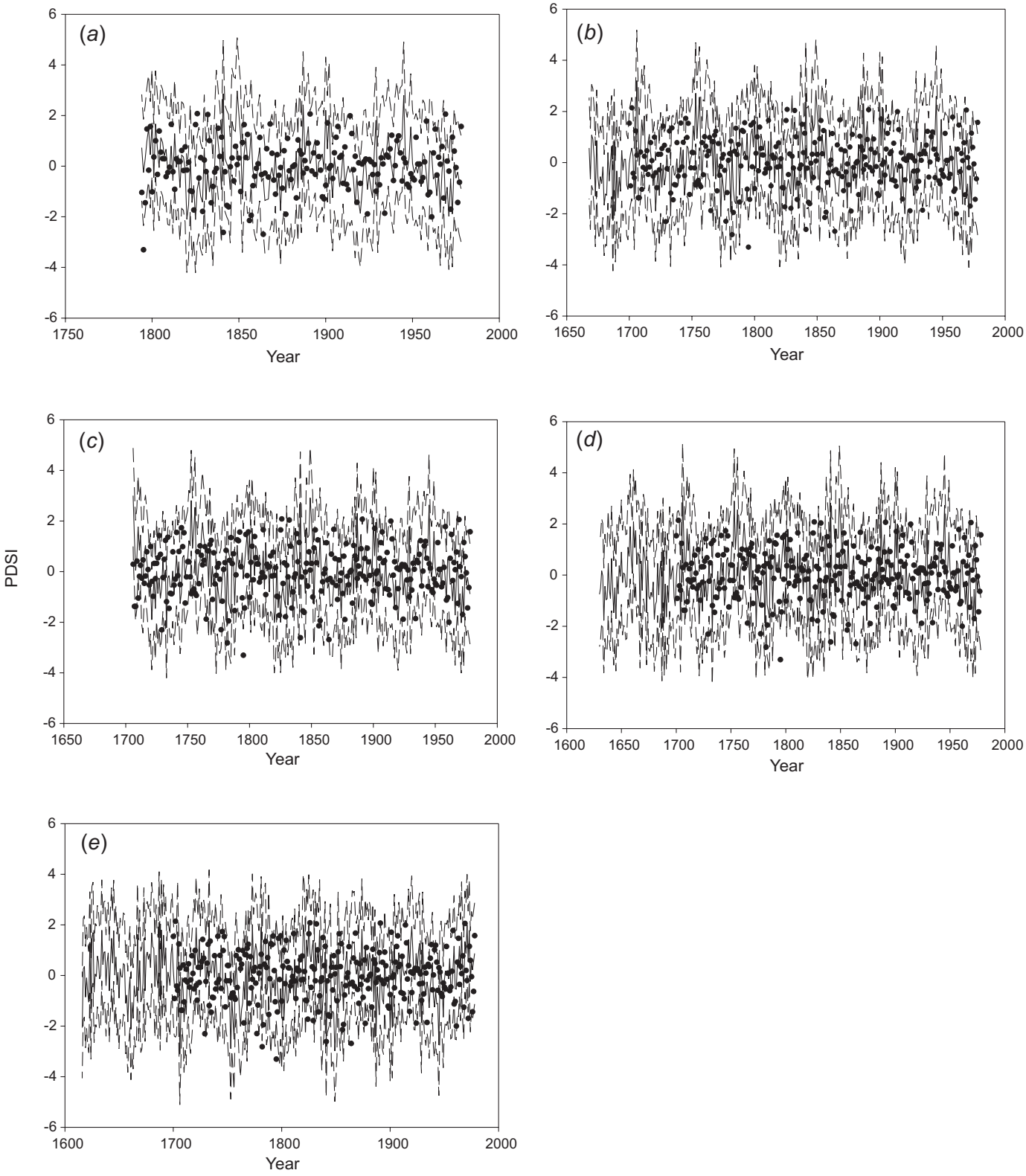

The 1, 2, 3, 5, 10, and 15 year time-lag models for white fir, red fir, incense cedar, and sugar pine had higher Δ_i values than the nonlagged models suggesting the best fit for these species was between the radial increment and PDSI value in the same year. For Jeffrey pine, the 5 year lag had the lowest AIC_c value (Table 3, Fig. 3). However, the 1, 2, 3, and 10 year time lags had Δ_i values within two of the 5 year lag, indicating that they were equally well supported.

Fig. 3. Kalman filter predictions (solid lines) with 95% confidence intervals (broken lines) and PSDI values (●) for Jeffrey pine increment growth lagged 5 years.

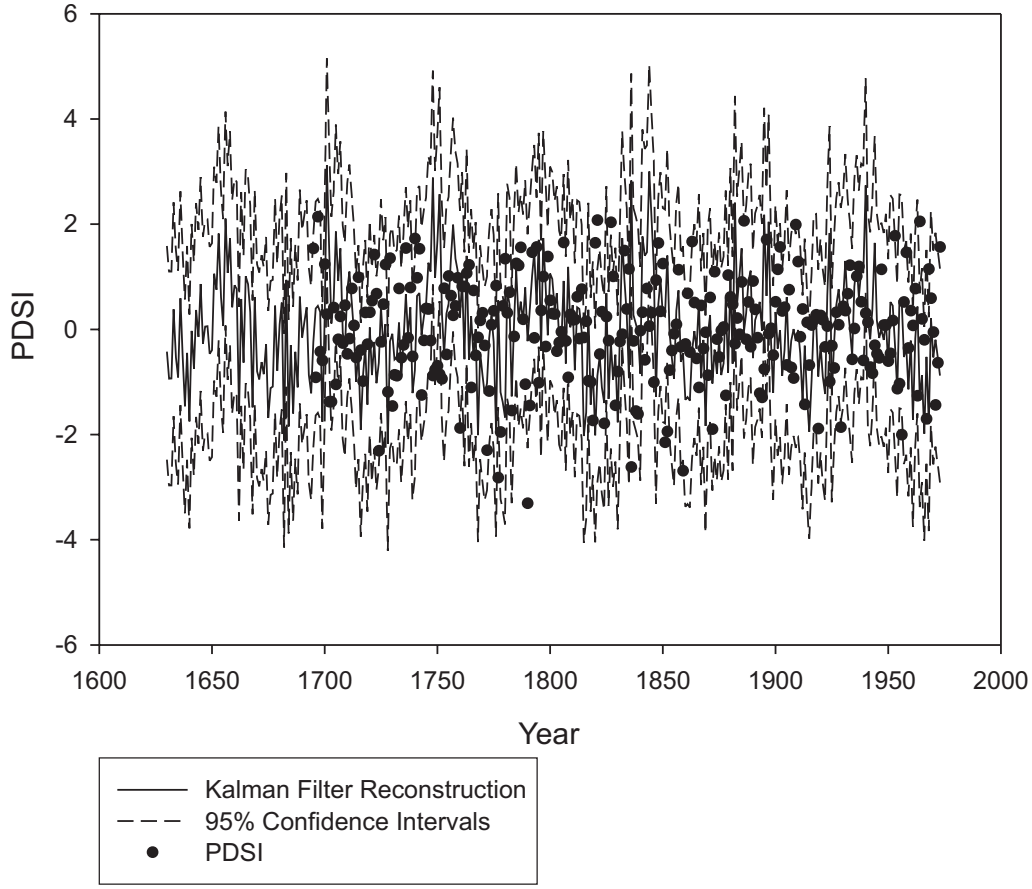

The 1, 2, 3, 5, and 10 year time-lag models represented 93% of the total weight (w_i) among models (Table 3). The 15 year lag and zero time lag models had less support as indicated by the evidence ratios (Table 3).

To examine the affects of density on annual growth for four mixed-conifer species (white fir, incense cedar, Jeffrey pine, and sugar pine), we used the tree map data set from the Teakettle project. We filtered a subset of individuals and determined that individuals with a weighted Thiessen value ≥41.25, which is equivalent to a spacing of 9 m between stems for a group of 50 cm trees, had consistently lower AIC_c values than individuals with Thiessen values <41.25 for white fir, incense cedar, Jeffrey pine, and sugar pine. Larger Thiessen values are associated with lower density. This finding indicates that individuals of each species growing in more open stand conditions have a stronger climate signal in annual growth rings than individuals of the same species growing in closed stands. A graph of Thiessen polygon size plotted against AIC_c for each sample tree (Fig. 4), with dummy variable regression lines overlain on the plot indicates that more open grown individuals (larger Thiessen value) have a stronger relationship (lower AIC_c values) between radial growth and annual climate. Comparing the slopes of the regression lines indicates that, once the Thiessen threshold is surpassed, there is a significant relationship between Thiessen value and AIC_c value (p = 0.0355). Although a Thiessen value of less than 50 did not always mean that the individual had a Δ_i value greater than 2, most of these recorder trees were poor indicators of climate. For red fir, density of the recorder tree was not related to the fit between PDSI and radial increment growth.

Discussion

When examining species-specific response to climate, we found that white fir had the lowest AIC_c value (–5.01), indicating that, of the selected models, white fir radial growth most accurately followed annual changes in PDSI. Species-specific differences in growth response to climate have also been documented in the dry forests of Namibia (Fichtler et al. 2004) and in high-elevation forests of the Sierra Nevada (Graumlich 1993). Fichtler et al. (2004) found that *Burkea africana* Hook. was more sensitive to precipitation than *Pterocarpus angolensis* DC. Graumlich (1993) found differences in growth response to climate between *Pinus balfouriana* Grev. & Balf. and *Juniperus occidentalis* Hook.

We found a density threshold where individuals that had larger Thiessen values (more open grown) tended to have Δ_i values within two of the best model (i.e., were better climate "recorders"). Density affects annual growth response in most tree species and often dampens or obscures the radial growth and climate relationship (Piutti and Cescatti 1997). In our sample, there were some open-grown trees that were not good recorders of annual climate conditions; with the variables we measured, we were unable to determine why these individuals did poorly.

Fig. 4. Thiessen polygon sizes plotted against the AIC_c values for a subset of individual trees for white fir (ABCO), incense cedar (CADE), Jeffrey pine (PIJE), and sugar pine (PILA). Regression lines from a dummy variable regression are included for the subset of individuals both above and below the Thiessen threshold value of 41.25. Individuals with Thiessen ≥41.25 had AIC_c values within 2 of the best model for a given species, indicating that they are equally well supported. Individuals with the lowest AIC_c values are the best models. A contrast of the slopes of the regression lines shows a significant difference in slopes ($p = 0.0355$).

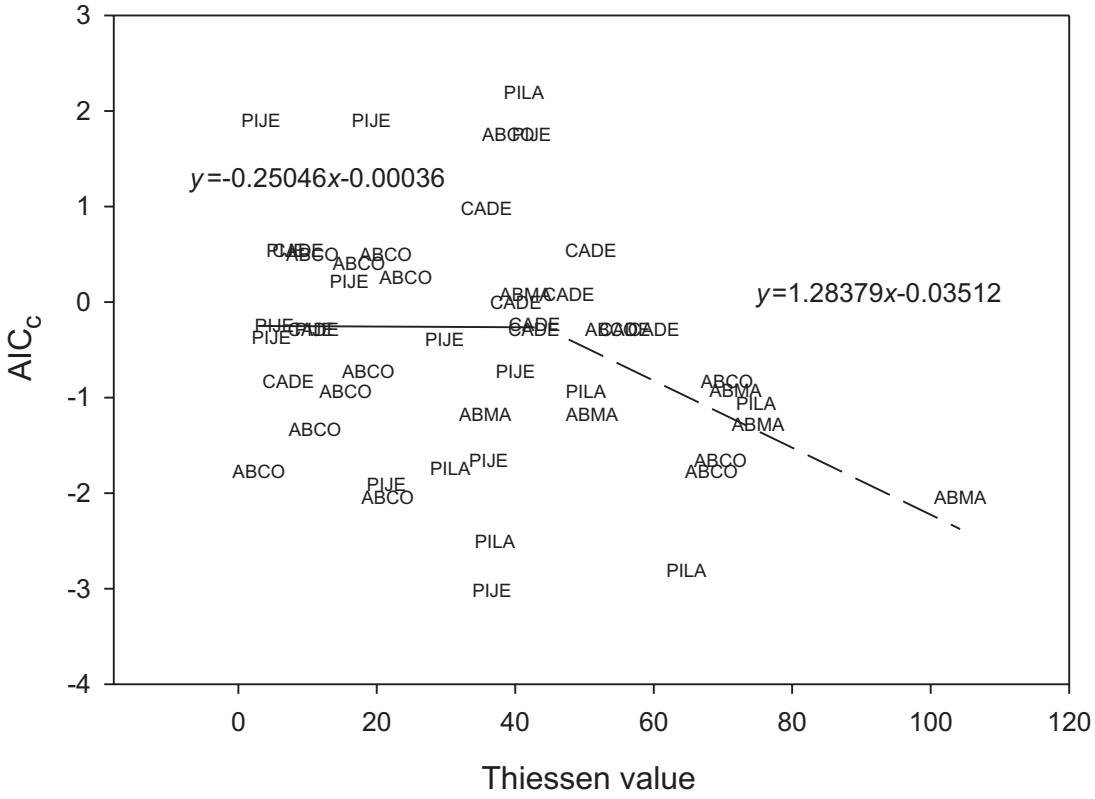

These results should be considered within the limitations of our study. By collecting cookies in close proportion to Teakettle's mixed-conifer composition, we have a much larger sample size for white fir and incense cedar than for red fir, Jeffrey pine, and sugar pine. We took this approach so that our sample was proportional to the stem frequency of the different species, but it also means we have a more robust model for white fir and incense cedar than the other species. Our analysis of whether local density may affect a tree's climate response assumes current conditions are representative of a tree's competitive environment over the period we analyzed and that all trees are competing for the same resources. Tall, deeply rooted, old-growth individuals may be only slightly affected by the close proximity of smaller, more shallow-rooted individuals. Demographic work at Teakettle (North et al. 2005) suggests current stem densities reflect the ingrowth of many small trees originating 15 years after Teakettle's last widespread fire in 1865. However, a recorder tree may have been influenced by adjacent trees that have died, decayed, and are no longer detectable in current stand conditions. Although many studies have found a strong influence of climate on annual radial growth (Douglass 1920; Fichtler et al. 2004; Graumlich 1993), changes in microsite conditions also influence radial increment growth and are difficult to identify and isolate from climate effects (Briffa et al. 1998*b*; Oberhuber and Kofler 2000; Tardif et al. 2003).

White fir annual radial growth was the best indicator of annual climate of the trees we sampled possibly because of its autecology and favored microsite conditions. White fir is often growing in clusters of trees, is found topographically in midslope stands, and is a strong shade-tolerant competitor (Harlow et al. 1996; Stuart and Sawyer 2001). These factors may be allowing white fir to capitalize on available moisture resulting in increased responsiveness to interannual fluctuations in precipitation. In our study, 67% of the white fir sampled had heights (10–25 m) that placed them in the midcanopy position. Gersonde and O'Hara (2005) found that individuals growing in the midcanopy had higher light use efficiencies than individuals growing in the lower or upper canopy. In addition, only 21% of the individuals we sampled were established prior to Teakettle's last extensive fire (1865). Seymour and Kenefic (2002) found that tree growth efficiency decreases with age. With a large majority of the white fir individuals sampled having established fairly recently, higher growth efficiency may contribute to their stronger growth–climate relationship.

Incense cedar growth was less correlated with annual climate than white fir, possibly because its light use efficiency does not differ with canopy position (Gersonde and O'Hara 2005) and because it does not experience accelerated growth during any of its life stages. incense cedar allocates a greater proportion of its growth to nonphotosynthetic tissue and, compared with white fir, has much thicker bark and larger branches. Mäkelä (1986) and Givnish (1988) found that a de-

crease in tree growth efficiency occurs as growth is concentrated in nonphotosynthetic tissue compared with leaf area.

Sugar pine was also less correlated with annual climate than white fir possibly because of its relatively plastic response to environmental conditions. Sugar pine can be shade tolerant in the seedling and sapling stages but becomes more shade intolerant with age (Harlow et al. 1996). In our study site, it occurs in xeric to mesic microsites. In addition to sugar pine's adaptability, 31% of our sample came from older trees (before 1865), which may have lower growth efficiency.

Red fir's poor growth–climate relationship may result from its topographic location within the mixed-conifer zone at the Teakettle Experimental Forest. Growing primarily within riparian zones (North et al. 2002), our red fir samples may have had a buffered microclimate, thereby reducing its sensitivity to annual climate fluctuations.

The relatively poor relationship between annual growth and climate for Jeffrey pine was unexpected, because North et al. (2005) found Jeffrey pine establishment associated with El Niño events at the same site. Jeffrey pine dominated stands are typically found on xeric south- or west-facing slopes and are characterized by open canopies and low stand densities (Rundel et al. 1977; Barbour and Minnich 2000). Most of Teakettle's Jeffrey pines are located in similar conditions. Open-grown trees tend to have lower growth variability associated with stand dynamics; whereas the xeric shallow-soiled sites Jeffrey pine occupies suggest these trees would be sensitive to precipitation (Schweingruber et al. 1990). Fekedulegn et al. (2003) has suggested species having a conservative growth strategy are less affected by drought than more rapidly growing individuals. Orwig and Abrams (1997) also have found that individuals growing on xeric sites were less impacted by drought than individuals growing in more mesic areas. However, in our study, some Jeffrey pine still had high annual growth rates even on xeric sites. A study by Hubbert et al. (2001) suggests Jeffrey pine might be buffered from annual precipitation abundance, because its roots can access deep water reservoirs. Working in a Jeffrey pine plantation in the southern Sierra, Hubbert et al. (2001) found that, throughout the growing season, Jeffrey pine extracted water from both the soil and bedrock fissures, and reliance on bedrock water increased as soil water was depleted. To inferentially examine this idea, we ran time-lagged models for each species, but only the Jeffrey pine model was substantially improved with a time lag model. Our study did not investigate the mechanisms that cause this delay, but one explanation might be Jeffrey pine's use of bedrock water, which buffers against current climate conditions but becomes exhausted during extended periods of drought. Although the possibility does exist that the lagged response may be the result of extreme weather events such as El Niño, these events are accounted for in the PDSI. The poor performance of lagged models for the other three species suggests annual growth is responding to extreme weather events in the year of occurrence. The relationship between Jeffrey pine seedling establishment and El Niño (North et al. 2005) may diminish over time as the root structure of adult trees grows and is able to access groundwater.

Unexpectedly, we found radial growth of a shade-tolerant species (white fir) correlated best with modern climate conditions and that, for one (red fir) of the five species sampled, open growing conditions did not improve climate model fit. As forest conditions become increasingly dense from a century of fire suppression, it may become more difficult to identify species and individuals that can provide the best annual growth to climate response. Our findings suggest that a tree's annual growth response to climate can be influenced by its species characteristics and localized differences in stand density.

Acknowledgements

The USDA Forest Service Pacific Southwest Sierra Nevada Research Center provided funding for this study. We thank Jason Jimenez for his help with field work; Jim Innes for help with logistics; Emilio Laca, University of California at Davis, for statistical consultation; and the Sierra National Forest for implementing thinning and burning treatments in the Teakettle Experiment.

References

Arkley, R.J. 1981. Soil moisture use by mixed conifer forest in a summer-dry climate. Soc. Soil Sci. Am. J. **45**: 423–427.

Akaike, H. 1973. Information theory as an extension of the maximum likelihood principle. *In* Second International Symposium on Information Theory, Budapest, Hungary. *Edited by* B.N. Petrov and F. Csaki. Akademiai Kiado, Budapest, Hungary. pp. 267–281.

Barbour, M.G., and Minnich, R.A. 2000. Californian uplands and woodlands. *In* North American terrestrial vegetation. 2nd ed. *Edited by* M.G. Barbour and W.D. Billings. Cambridge University Press, Cambridge, UK. pp. 161–202.

Biondi, F. 1996. Decadal-scale dynamics at the Gus Pearson Natural Area: evidence for inverse (a)symmetric competition? Can. J. For. Res. **26**: 1397–1406. doi:10.1139/x26-156.

Briffa, K.R., and Osborn, T.J. 1999. Seeing the wood from the trees. Science (Washington, D.C.), **284**: 926–927. doi:10.1126/science.284.5416.926.

Briffa, K.R., Schweingruber, F.H., Jones, P.D., Osborn, T.J., Shiyatov, S.G., and Vaganov, E.A. 1998*a*. Reduced sensitivity of recent tree-growth to temperature at high northern latitudes. Nature (London), **391**: 678–682. doi:10.1038/35596.

Briffa, K.R., Schweingruber, F.H., Jones, P.D., Osborn, T.J., Harris, I.C., Shiyatov, S.G., Vaganov, E.A., and Grudd, H. 1998*b*. Trees tell of past climates: but are they speaking less clearly today? Philos. Trans. R. Soc. Lond. B Biol. Sci. **353**: 65–73. doi:10.1098/rstb.1998.0191.

Burnham, K.P., and Anderson, D.R. 2002. Model selection and multimodel inference: a practical information-theoretic approach. 2nd ed. Springer, New York.

Cook, E.R., Meko, D.M., Stahle, D.W., and Cleaveland, M.K. 1999. Drought reconstructions for the continental United States. J. Clim. **12**: 1145–1162. doi:10.1175/1520-0442(1999)012<1145:DRFTCU>2.0.CO;2.

du Plessis, R.M. 1996. Poor man's explanation of Kalman filtering or how I stopped worrying and learned to love matrix inversion. Taygeta Scientific Inc., Monterey, Calif.

Douglass, A.E. 1920. Evidence of climatic effects in the annual rings of trees. Ecology, **1**: 24–32. doi:10.2307/1929253.

Fekedulegn, D., Hicks, R.R., and Colbert, J.J. 2003. Influence of topographic aspect, precipitation and drought on radial growth of four major tree species in an Appalachian watershed. For. Ecol. Manage. **177**: 409–425. doi:10.1016/S0378-1127(02)00446-2.

Fichtler, E., Trouet, V., Beeckman, H., Coppin, P., and Worbes, M. 2004. Climatic signals in tree rings of *Burkea africana* and *Pterocarpus angolensis* from semiarid forests in Namibia. Trees (Berl.), **18**: 442–451. doi:doi:10.1007/s00468-004-0324-0.

Gersonde, R.F., and O'Hara, K.L. 2005. Comparative tree growth efficiency in Sierra Nevada mixed-conifer forests. For. Ecol. Manage. **219**: 95–108. doi:10.1016/j.foreco.2005.09.002.

Givnish, T.J. 1988. Adaptation to sun and shade: a whole-plant perspective. Aust. J. Plant Physiol. **15**: 63–92.

Gove, J.H., and Houston, D.R. 1996. Monitoring the growth of American beech affected by beech bark disease in Maine using the Kalman filter. Environ. Ecol. Stat. **3**: 167–187. doi:10.1007/BF02427860.

Graumlich, L.J. 1993. A 1000-year record of temperature and precipitation in the Sierra Nevada. Quat. Res. **39**: 249–255. doi:10.1006/qres.1993.1029.

Harlow, W.W., Harrar, E.S., Hardin, J.W., and White, F.M. 1996. Textbook of dendrology. 8th ed. McGraw-Hill Inc., New York.

Holmes, R.L., Adams, R.K., and Fritts, H.C. 1986. Tree-ring chronologies of western North America: California, wastern Oregon and northern Great Basin. Laboratory of Tree-Ring Research, University of Arizona, Tucson, Ariz.

Hubbert, K.R., Beyers, J.L., and Graham, R.C. 2001. Roles of weathered bedrock and soil in seasonal water relations of *Pinus jeffreyi* and *Arctostaphylos patula*. Can. J. For. Res. **31**: 1947–1957. doi:10.1139/cjfr-31-11-1947.

Kalman, R.E. 1960. A new approach to linear filtering and prediction problems. Trans. ASME. Ser. D J. Basic Eng. **82**: 35–45.

Kenkel, N.C., Hoskins, J.A., and Hoskins, W.D. 1989. Local competition in a naturally established jack pine stand. Can. J. Bot. **67**: 2630–2635. doi:10.1139/cjb-67-9-2630.

Kiladis, G.N., and Diaz, H.F. 1989. Global climatic anomalies associated with extremes in the Southern Oscillation. J. Clim. **2**: 1069–1090. doi:10.1175/1520-0442(1989)002<1069:GCAAWE>2.0.CO;2.

Mäkelä, A. 1986. Implications of the pipe model theory on dry matter partitioning and height growth in trees. J. Theor. Biol. **123**: 103–120. doi:10.1016/S0022-5193(86)80238-7.

Maybeck, P.S. 1979. Stochastic models, estimation, and control. Vol. 1. Academic Press, New York.

McKelvey, K.S., and Busse, K.K. 1996. Twentieth-century fire patterns on forest service lands. *In* Sierra Nevada Ecosystem Project, Final Report to Congress. Centers for Water and Wildland Resources, University of California, Davis, Calif.

Mithen, R., Harper, J.L., and Weiner, J. 1984. Growth and mortality of individual plants as a function of "available area." Oecologia, **62**: 57–60. doi:10.1007/BF00377373.

Muir, J. 1894. The mountains of California. The Century Co, New York.

North, M., Oakley, B., Chen, J., Erickson, H., Gray, A., Izzo, A., Johnson, D., Ma, S., Marra, J., Meyer, M., Purcell, K., Rambo, T., Rizzo, D., Roath, B., and Schowalter, T. 2002. Vegetation and ecological characteristics of mixed-conifer and red-fir forests at the Teakettle Experimental Forest. USDA For. Serv. Gen. Tech. Rep. PSW-GTR-186.

North, M., Chen, J., Oakley, B., Song, B., Rudnicki, M., Gray, A., and Innes, J. 2004. Forest stand structure and pattern of old-growth western hemlock/Douglas-fir and mixed-conifer forest. For. Sci. **50**: 299–311.

North, M., Hurteau, M., Fiegener, R., and Barbour, M. 2005. Influence of fire and El Niño on tree recruitment varies by species in Sierran mixed conifer. For. Sci. **51**: 187–197.

Oberhuber, W., and Kofler, W. 2000. Topographic influences on radial growth of Scots pine (*Pinus sylvestris* L.) at small spatial scales. Plant Ecol. **146**: 229–238. doi:doi:10.1023/A:1009827628125.

Orwig, D.A., and Abrams, M.D. 1997. Variation in radial growth responses to drought among species, site, and canopy strata. Trees (Berl.), **11**: 474–484. doi:doi:10.1007/s004680050110.

Palmer, W.C. 1965. Meteorological drought. US Department of Commerce, Washington, D.C. Weather Bur. Res. Pap. No. 45.

Pan, Y., and Raynal, D.J. 1995. Predicting growth of plantation conifers in the Adirondack Mountains in response to climate change. Can. J. For. Res. **25**: 48–56. doi:10.1139/cjfr-25-1-48.

Peterman, R.M., Pyper, B.J., and MacGregor, B.W. 2003. Use of the Kalman filter to reconstruct historical trends in productivity of Bristol Bay sockeye salmon (*Oncorhynchus nerka*). Can. J. Fish. Aquat. Sci. **60**: 809–824. doi:10.1139/f03-069.

Piutti, E., and Cescatti, A. 1997. A quantitative analysis of the interactions between climatic response and intraspecific competition in European beech. Can. J. For. Res. **27**: 277–284. doi:10.1139/cjfr-27-3-277.

Rundel, P.W., Gordon, D.T., and Parsons, D.J. 1977. Montane and subalpine vegetation of the Sierra Nevada and Cascade Ranges. *In* Terrestrial vegetation of California. *Edited by* M.G. Barbour and J. Major. John Wiley & Sons, Inc, New York. pp. 559–599.

Schweingruber, F.H., Kairiukstis, L., and Shiyatov, S. 1990. Sample selection. *In* Methods of dendrochronology: applications in the environmental sciences. *Edited by* E.R. Cook and L.A. Kairiukstis. Kluwer Academic Publishers, Dordrecht, the Netherlands. pp. 23–35.

Seymour, R.S., and Kenefic, L.S. 2002. Influence of age on growth efficiency of *Tsuga canadensis* and *Picea rubens* trees in mixed-species, multiaged northern conifer stands. Can. J. For. Res. **32**: 2032–2042. doi:10.1139/x02-120.

Shumway, R.H., and Stoffer, D.S. 2000. Time series analysis and its applications. Springer-Verlag, New York.

Smith, C.A., and Sardeshmukh, P. 2000. The effect of ENSO on the intraseasonal variance of surface temperatures in winter. Int. J. Climatol. **20**: 1543–1557. doi:10.1002/1097-0088 (20001115) 20:13<1543::AID-JOC579>3.0.CO;2-A.

Steele, B., and Fiedler, C. 1996. Kalman filter analysis of growth–climate relations in old-growth ponderosa pine/Douglas-fir stands. *In* Tree Rings, Environment and Humanity, 17–21 May 1994, Tucson, Ariz. *Edited by* J.S. Dean, D.M. Meko, and T.W. Swetnam. Department of Geosciences, University of Arizona, Tucson, Ariz. pp. 303–314.

Stephens, S.L., and Elliot-Fisk, D.L. 1998. *Sequoiadendron giganteum* – mixed conifer forest structure in 1900–1901 from the southern Sierra Nevada, CA. Madrono, **45**: 221–230.

Stokes, M.A., and Smiley, T.L. 1968. An introduction to tree-ring dating. University of Chicago, Chicago, Ill.

Stuart, J.D., and Sawyer, J.O. 2001. Trees and shrubs of California. University of California Press, Berkeley, Calif.

Tardif, J., Camarero, J.J., Ribas, M., and Gutierrez, E. 2003. Spatiotemporal variability in tree growth in the central Pyrenees: climatic and site influences. Ecol. Monogr. **73**: 241–257. doi:10.1890/0012-9615(2003)073[0241;SVIGTI]2.0.CO;2.

van den Brakel, J.A., and Visser, H. 1996. The influence of environmental conditions on tree-ring series of Norway spruce for different canopy and vitality classes. For. Sci. **42**: 206–219.

Van Deusen, P.C. 1990. Evaluating time-dependent tree ring and climate relationships. J. Environ. Qual. **19**: 481–488.

Van Deusen, P.C., and Koretz, J. 1988. Theory and programs for dynamic modeling of tree rings and climate. USDA For. Serv. Gen. Tech. Rep. SO-70.

Wilmking, M., Juday, G.P., Barber, V.A., and Zald, H.S.J. 2004.

Recent climate warming forces contrasting growth responses of white spruce at treeline in Alaska through temperature thresholds. Glob. Change Biol. **10**: 1724–1736. doi:10.1111/j.1365-2486.2004.00826.x.

Witty, J.H., Graham, R.C., Hubbert, K.R., Doolittle, J.A., and Wald, J.A. 2003. Contributions of water supply from the weathered bedrock zone to forest soil quality. Geoderma, **114**: 389–400. doi:10.1016/S0016-7061(03)00051-X.

Yamaguchi, D.K. 1991. A simple method for cross-dating increment cores from living trees. Can. J. For. Res. **21**: 414–416. doi:10.1139/cjfr-21-3-414.